Haem is involved in the NO-mediated regulation by *Bradyrhizobium diazoefficiens* NnrR transcription factor

Andrea Jiménez-Leiva[a], Juan J. Cabrera[a], María J. Torres[a,1], David J. Richardson[b], Eulogio J. Bedmar[a], Andrew J. Gates[b], María J. Delgado[a,*], S. Mesa[a,*]

[a] *Department of Soil and Plant Microbiology, Estación Experimental del Zaidín, CSIC, 18008 Granada, Spain*

[b] *School of Biological Sciences, University of East Anglia, Norwich Research Park, Norwich NR4 7TJ, United Kingdom*

[1] Present address:
Department of Biochemistry and Molecular Biology, Campus Universitario de Rabanales, University of Córdoba, Ed. C6, Planta Baja, 14071 Córdoba, Spain

[*] Correspondence to:
Department of Soil and Plant Microbiology, Estación Experimental del Zaidín, CSIC, 18008 Granada, Spain. *E-mail addresses*: mariajesus.delgado@eez.csic.es (M.J. Delgado), socorro.mesa@eez.csic.es (S. Mesa)

E-mail addresses:
andrea.jimenez@eez.csic.es (A. Jiménez-Leiva)
juan.cabrera@eez.csic.esca (J.J. Cabrera)
bb2topom@uco.es (M.J. Torres)
D.Richardson@uea.ac.uk (D.J. Richardson)
eulogio.bedmar@eez.csic.es (E.J. Bedmar)
A.Gates@uea.ac.uk (A.J. Gates)
mariajesus.delgado@eez.csic.es (M.J. Delgado)
socorro.mesa@eez.csic.es (S. Mesa)

ABSTRACT

Nitric oxide (NO) and the greenhouse (GHG) gas nitrous oxide (N_2O) contribute significantly to climate change. In rhizobia, the denitrifying enzyme *c*-type nitric oxide reductase (cNor), encoded by *norCBQD* genes, is crucial for maintaining a delicate balance of NO and N_2O levels. In the soybean endosymbiont *Bradyrhizobium diazoefficiens,* maximal expression of *norCBQD* genes in response to NO is controlled by NnrR, which belongs to a distinct clade of the CRP/FNR family of bacterial transcription factors. This protein participates in the FixLJ-$FixK_2$-NnrR regulatory cascade that induces denitrification genes expression in response to oxygen limitation and nitrogen oxides. However, the molecular mechanism underpinning NO sensing by *B. diazoefficiens* NnrR has remained elusive. Here, we revealed that NnrR induces *norCBQD* gene expression in response to NO uncoupled from the superimposed $FixK_2$ control. Moreover, NO-mediated induction by NnrR is dependent on haem, as the expression of a *norC-lacZ* fusion was impaired in a *hemN_2* mutant defective in haem biosynthesis. *In vitro* studies showed that NnrR bound haem with a 1:1 stoichiometry (monomer:haem), according to titration experiments of recombinant NnrR protein with hemin performed under anaerobic conditions. Furthermore, the full UV-Visible spectra of haem-reconstituted NnrR showed a peak at 411 nm (ferric form), and at 425 nm (ferrous derivative). This latter complex was able to bind NO under anaerobic conditions. Finally, we performed a functional mutagenesis of specific residues in NnrR predicted as putative ligands for haem binding. While H11 was important for *norC* expression and Nor activity, a H11A-H56A protein variant showed a reduced affinity for haem binding. Taken together, our results identify haem as the cofactor for NnrR-mediated NO sensing in *B. diazoefficiens* denitrification, with H11 as a key residue for NnrR function, providing the first insight into the mechanism of an NnrR-type protein. These findings advance our understanding of how bacterial systems orchestrate the denitrification process and respond to environmental cues such as NO.

Keywords

Cofactor, CRP/FNR proteins, denitrification, rhizobia, sensing domain, transcription

Abbreviations

CRP/FNR, cyclic AMP receptor protein/fumarate and nitrate reductase regulator; cPTIO, (2-4-carboxyphenyl-4,4,5,5-tetramethylimidazoline-1-oxyl-3-oxide); CBD, chitin-binding domain; DNR, dissimilative nitrate respiration regulator; GHG, greenhouse gas; IMPACT, intein-mediated purification with an affinity chitin-binding tag; IPTG, isopropyl β-D-1-

thiogalactopyranoside; Nap, periplasmic nitrate reductase; Nir, nitrite reductase; NnrR, nitrite and nitric oxide reductase regulator; cNor, nitric oxide reductase type *c*; Nos, nitrous oxide reductase; OD, optical density; PDB, Protein Data Bank; PSY, peptone-salts-yeast extract; SDS-PAGE, sodium dodecyl sulphate-polyacrylamide gel electrophoresis; UV-Vis, ultraviolet-visible; WT, wild type; YEM, yeast extract-mannitol; YEMN, yeast extract-mannitol nitrate.

Highlights

- NnrR activates *norCBQD* expression in response to NO uncoupled from $FixK_2$ control
- Haem is involved in NnrR-mediated NO sensing *in vivo*
- NnrR-ferrous haem complex binds NO *in vitro*
- H11 is relevant for NnrR regulation of *B. diazoefficiens* cNor
- The NO-sensing mechanism of an NnrR-type protein was revealed for the first time

1. Introduction

Nitric oxide (NO) is a reactive gas that, depending on its concentration, has multiple functions in biological systems. At low concentrations, NO is a signalling molecule, while at high concentrations, it becomes highly toxic due to its capacity to react with numerous cellular targets (Toledo and Augusto, 2012). NO also plays an important role in atmospheric chemistry and is a precursor of the potent greenhouse gas (GHG) nitrous oxide (N_2O).

Denitrification is currently considered to be the main respiratory source of NO. This molecule is a key intermediate in the denitrification pathway by which nitrate (NO_3^-) or nitrite (NO_2^-) is sequentially reduced via NO and N_2O to molecular nitrogen (N_2) for respiration under low-oxygen conditions (Zumft, 1997). The four denitrification steps are catalysed by a periplasmic nitrate reductase (Nap) or a membrane-associated nitrate reductase (Nar), nitrite reductases (NirK or NirS), nitric oxide reductases (cNor, qNor or Cu_ANor) and a nitrous oxide reductase (NosZ) encoded by the *nap/nar*, *nir*, *nor* or *nos* genes, respectively (van Spanning et al., 2007; Richardson, 2011; Bueno et al., 2012; Torres et al., 2016; Salas et al., 2021). All of these enzymes are linked to the respiratory electron transport chain, of which Nap, NirS and cNor contain haem as a cofactor (Salas et al., 2021).

As NO is a potent cytotoxin and a source of N_2O, both NO-producing (Nir) and NO-consuming (Nor) enzymes must be very tightly controlled to avoid NO accumulation and N_2O emissions. In this context, several NO-responsive transcription factors have been proposed to regulate denitrification genes involved in NO balance (Spiro, 2007, 2011; Stern and Zhu, 2014; Torres et al., 2016). In particular, NnrR (nitrite and nitric oxide reductase regulator) and DNR (dissimilative nitrate respiration regulator) proteins are distinct clades of the cyclic AMP (cAMP) receptor protein (CRP)/fumarate and nitrate reductase regulator (FNR) family of transcription factors that respond to a wide variety of intra- and extracellular cues (Körner et al., 2003; Dufour et al., 2010; Matsui et al., 2013). In this family of regulators, signal transduction occurs through an interaction between the specific molecule and the sensory domain of the protein, which induces a conformational change that leads to the binding of the active dimer to a specific DNA sequence located at the promoter region of target genes (Browning and Busby, 2004; Dufour et al., 2010).

Haem has been recognised as a cofactor in many biological molecules due to its versatility. In particular, *b*- and *c*-type haem, derived from protoporphyrinogen IX, are the most common groups associated with sensor proteins. Often, haem binds to the N-terminus, embedded in a

hydrophobic pocket that is not accessible to solvents, while the C-terminus contains the functional domain. The extraordinary redox chemistry of haem is used by bacterial haem-containing proteins to sense and respond to varying levels of diatomic gas molecules such as CO, NO, and O_2 to play critical roles in biological processes, including respiration, metabolism, O_2 transport, regulation of gene expression, and others (Farhana et al., 2012; Fonseca et al., 2013).

In particular, the perception of NO by *Pseudomonas aeruginosa* DNR, that triggers protein-DNA binding and transcription activation of *nir* and *nor* genes, requires haem (Castiglione et al., 2009). Indeed, recombinant DNR is able to bind haem *in vitro* (Giardina et al., 2008), and a hydrophobic pocket has been identified in the crystal structure of this protein as a putative haem-binding site (Giardina et al., 2009). Especially, a histidine residue (H187) located in the distal part of this haem pocket is directly involved in iron coordination, in combination with a second residue (probably H14 or H15) required for haem-binding stabilisation (Rinaldo et al., 2012; Cutruzzolá et al., 2014). Similarly, DnrF from *Dinoroseobacter shibae*, another DNR-type protein, senses NO via its bound haem cofactor and induces the expression of the NO reductase genes (*norCB*) (Ebert et al., 2017). However, the key histidine residues of *P. aeruginosa* DNR required for haem coordination and stabilisation are not conserved in *D. shibae* DnrF. In contrast to the DNR clade, very little is known about the NO sensing mechanism by the NnrR clade proteins.

Bradyrhizobium diazoefficiens, the soybean endosymbiont, is considered a model to study denitrification in rhizobia where is carried out by four enzymatic steps through a Nap, a copper-containing NirK, a cNor, and a NosZ (Bedmar et al., 2005). In this bacterium, this pathway is controlled by two interconnected regulatory cascades (FixLJ-$FixK_2$-NnrR and RegSR-NifA), both of which respond to low-oxygen conditions (Fernández et al., 2016; Torres et al., 2016; Salas et al., 2021). Specifically, in the FixLJ-$FixK_2$-NnrR cascade, the low O_2 signal is perceived by the haem-based sensor protein FixL that autophosphorylates and transfers the phosphoryl group to the response regulator FixJ, which in turn, activates the expression of the *$fixK_2$* gene that encodes the $FixK_2$ protein. The NnrR regulator, which is directly controlled by the superimposed transcription factor $FixK_2$ (Jiménez-Leiva et al., 2019), is required for the maximal expression of the *norCBQD* genes in response to NO (Bueno et al., 2017), similar to that described in another rhizobia (Cabrera et al., 2011). Furthermore, recombinant NnrR protein was able to interact with the *norCBQD* promoter *in vitro* under anaerobic conditions (Bueno et al., 2017). The mutual dependence of NO and NnrR for *norCBQD* genes expression

suggests a role for *B. diazoefficiens* NnrR as an NO-responsive transcriptional activator. However, the molecular mechanism underlying NO sensing by NnrR is still unknown.

In *B. diazoefficiens*, the *hemN*$_2$ gene encodes a coproporphyrinogen III dehydrogenase that catalyses the conversion of protoporphyrinogen III to protoporphyrinogen IX, which is involved in the haem biosynthetic pathway under anaerobic conditions in this bacterium. Interestingly, a *hemN*$_2$ mutant failed to fix nitrogen in symbiosis with the soybean host plant and was also unable to grow under denitrifying conditions and showed reduced levels of NorC (Fischer et al., 2001). The latter two observations suggest that haem synthesis by HemN$_2$ is crucial for denitrification in *B. diazoefficiens*.

In the present work, we aimed to improve the understanding of the regulatory mechanisms governing denitrification in *B. diazoefficiens*, with a particular focus on the expression of *norCBQD* genes encoding cNor, in response to NO via the NnrR transcription factor. We therefore applied a multidisciplinary approach *in vivo* and *in vitro* which revealed *B. diazoefficiens* NnrR as a haem-dependent NO sensor. The molecular mechanism of *B. diazoefficiens* NnrR provides insights into other NO-sensing proteins and thus broadens the range of possibilities on how activity of CRP/FNR-type transcription factors can be modulated. This knowledge could be leveraged to devise strategies for engineering microbial processes, including NO consumption and N_2O production through denitrification, with a view to biotechnological or environmental applications that mitigate atmospheric GHG emissions in agricultural systems.

2. Materials and methods

2.1. Media, and growth conditions

Peptone Salts Yeast extract (PSY) complete medium supplemented with 0.1% L-arabinose (Regensburger and Hennecke, 1983; Mesa et al., 2008) was used for routine cultures of *B. diazoefficiens* strains as it is the standard medium usually employed for this purpose. Cells were incubated aerobically at 30 ºC under vigorous shaking (170 rpm) for 4 days. Yeast extract-mannitol (YEM) complete medium (Daniel and Appleby, 1972) was selected to cultivate cells under microaerobic and anaerobic conditions. Cultures for β-galactosidase activity assays, haem-staining experiments, and NO consumption were incubated under microaerobic (2% O_2, 98% N_2) or anaerobic conditions (filled tube) basically as described elsewhere (Bueno et al., 2017; Torres et al., 2017; Cabrera et al., 2021). For β-galactosidase activity assays, 17-ml rubber

stoppered tubes containing 3 ml (microaerobic conditions) or completely filled of YEM medium (anaerobic conditions) (Daniel and Appleby, 1972) were employed, while for haem-staining and NO consumption experiments, the volume of the cultures was 100 ml in 500 ml Erlenmeyer flasks (microaerobic conditions) or completely filled 100 ml flasks (anaerobic conditions). After inoculation at an initial optical density at 600 nm (OD_{600}) of 0.2, the cultures were incubated for 24 h, and exposed or not to 50 μM NO for 5 h. When needed, 1 mM of the NO-scavenger cPTIO (2-4-carboxyphenyl-4,4,5,5-tetramethylimidazoline-1-oxyl-3-oxide), hemin (15 μg/ml) or 10 mM KNO_3 was added from the beginning of the cultures. Denitrifying growth was monitored in filled, rubber stoppered 17-ml tubes containing YEM medium supplemented with 10 mM of KNO_3 (YEMN) that were inoculated at an initial OD_{600} of 0.02. When required, antibiotics were added at the following concentrations (in μg/ml): chloramphenicol, 15 (solid medium); spectinomycin, kanamycin and streptomycin, 200 (solid medium), 100 (liquid medium); tetracycline, 100 (solid medium), 50 (liquid medium).

LB medium was used for routine cultures of *E. coli* cells incubated at 37 ºC. *E. coli* ER2566 cells for overexpression of *B. diazoefficiens* NnrR protein derivatives were grown at 30 ºC. When needed, antibiotics were applied at the following concentrations (in μg/ml): ampicillin, 200; kanamycin, 30; spectinomycin, 25; streptomycin, 25; tetracycline, 10.

2.2. Strains and plasmids

The complete list of strains and plasmids used in this work is detailed in Table S1. Oligonucleotide names and sequences are compiled in Table S2.

Complementation of *fixK₂* and *nnrR* mutant strains with the *nnrR* gene was carried out using two different plasmids. The *nnrR* mutant was complemented with plasmid pRJ8845, which contains the *nnrR* gene expressed from its own promoter. The *fixK₂* mutant was complemented with plasmid pMB1407, which expresses the *nnrR* gene under the control of the constitutive *lacZ* promoter from the pBBR1MCS-2 vector. For the construction of this plasmid, a 770-bp fragment comprising 36 nucleotides upstream of the *nnrR* coding region, in order to preserve the genuine ribosome binding site, was amplified by PCR with oligonucleotides nnrR_7_for/rev. The PCR fragment was digested with *Kpn*I and *Bam*HI, and cloned into pBBR1MSC-2, yielding plasmid pMB1407. Next, plasmids pRJ8845 and pMB1407 were individually transferred by transformation into *E. coli* S17.1 cells which were used as donors in individual biparental matings with *nnrR* and *fixK₂* mutant strains. The verification of the

presence of each plasmid was carried out by PCR using as primer pairs' pPP375_for/rev and M13 for/rev for pRJ8845 and pMB1407, respectively.

The Intein Mediated Purification with an Affinity Chitin-binding Tag (IMPACT) system (New England Biolabs, NEB) was used to construct a battery of plasmids overexpressing different NnrR protein derivatives. For the parental NnrR protein, a 740-bp fragment containing the *nnrR* gene was amplified by PCR using primers nnrR-8_for/rev. This fragment was then digested with *Nde*I and *Bcu*I, and cloned into pTXB1 restricted with the same restriction enzymes, thus yielding plasmid pMB1122. Site-directed mutagenesis was employed to replace H11 and H56 in NnrR with alanine. For this purpose, plasmid pMB1122 and two sets of complementary primer pairs' (nnrR-H11A-for/rev and nnrR-H56A-for/rev) were used, yielding plasmids pMB1420 and pMB1421, respectively. Plasmid pMB1425 encoding the H11A-H56A NnrR protein variant was generated by site-directed mutagenesis using nnrR-H56A-for/rev primers and plasmid pMB1420.

The point mutations in NnrR were also prepared for introduction into *B. diazoefficiens*. First, the same site-directed mutagenesis strategy for the construction of the expression plasmids was applied using plasmid pJCR002 as template. This resulted in plasmids pMB1422 and pMB1423, encoding H11A and H56A NnrR protein derivatives. The construction of plasmid pMB1424 harbouring the *nnrR* gene with the double H11A/H56A mutation was based on the pMB1422 plasmid. Next, 1806-bp *Xba*I-*Hin*dIII fragments from pMB1422, pMB1423, and pMB1424 were individually cloned into the pK18*mobsacB* suicide vector cut with the same restriction enzymes, resulting in plasmids pMB1418, pMB1419, and pMB1426. These three plasmids were then individually transferred by conjugation from *E. coli* S17-1 cells to *B. diazoefficiens* Δ*nnrR* for markerless mutant construction using the *sacB*-system, and the selection of candidates was performed as described by Cabrera and colleagues (2016). The desired mutations were verified by PCR and sequencing. Three strains were thus obtained: 110*spc*4-001-1418 (encoding H11A NnrR), 110*spc*4-001-1419 (encoding H56A NnrR), 110*spc*4-001-1426 (encoding H11A-H56A NnrR).

In all cases, the fidelity of the amplified PCR fragments, the plasmid inserts, and the desired mutations was verified by sequencing.

2.3. β-galactosidase activity determination

The activity of NnrR *in vivo* was determined indirectly by measuring β-galactosidase activity of a *norC-lacZ* fusion in a series of *B. diazoefficiens* strains and conditions according to the

protocols described elsewhere (Miller 1972, Cabrera et al., 2021). The presence of the plasmid in the strains complemented *in trans* was verified by PCR at the end of each assay.

2.4. Haem c *proteins analyses*

NorC levels were estimated indirectly by detection of *c*-type membrane-bound cytochromes by the haem-staining methodology essentially as described by Jiménez-Leiva and coworkers (2019). Briefly, *B. diazoefficiens* cells were harvested and subsequently lysed using a French Press to obtain crude cell extracts. After ultracentrifugation, membrane fractions were obtained. Ten (10) µg of membrane suspensions were resolved on 14% SDS-PAGE gels and then transferred to a nitrocellulose membrane using a Trans-Blot Turbo System (Bio-Rad). Haem *c* proteins were detected based on their haem-dependent peroxidase activity using a ChemiDoc XRS+ System (Bio-Rad). The Image LabTM 6.1 software (Bio-Rad) was used for image analysis.

2.5. NO consumption activity

To determine NO consumption rates, *B. diazoefficiens* cells were subject to centrifugation at 7500 ×*g* for 10 min at 4 ºC, followed by two washes with 25 mM phosphate buffer at pH 7.4. The cell pellet was then resuspended in 1 ml of the same buffer to obtain a cell suspension with a protein concentration of 4–5 mg/ml. NO consumption was measured using a 2-mm ISONOP NO electrode APOLLO 4000® (World Precision Institute) under controlled temperature (30 ºC) and continuous stirring. The 2 ml-reaction chamber was loaded with 1.36 ml of 25 mM phosphate buffer (pH 7.4), 90 µl of 1 M sodium succinate, 100 µl of 320 mM glucose, 300 µl of the cell suspension, and 100 µl of an enzyme mixture containing 40 U/ml of *Aspergillus niger* glucose oxidase and 250 U/ml of bovine liver catalase (Sigma-Aldrich). A stable baseline was established before the addition of 50 µl of a saturated NO solution (1.91 mM at 20 ºC) to initiate the reaction. The assay was followed until NO detection dropped to zero, indicating complete consumption of NO.

2.6. Overproduction and purification of untagged NnrR proteins

Tag-free NnrR proteins were overexpressed and purified with the IMPACT system (NEB) following basically the protocol previously described (Cabrera et al., 2021; Tomás-Gallardo et al., 2024). Firstly, *E. coli* ER2566 competent cells were individually transformed with plasmids pMB1122, pMB1420, pMB1421, and pMB1425. For NnrR-*Mxe*-Intein-CBD proteins overproduction, cells were grown until an OD_{600} of 0.7 - 0.8, when 0.1 mM isopropyl-β-D-

thiogalactopyranoside (IPTG) was added, and then incubated for 2 h at 30 ºC. Cells harvest and protein purification were performed as described elsewhere (Tomás-Gallardo et al., 2024). The purity of the NnrR proteins was analysed by SDS-PAGE (Fig. S1).

2.7. Haem titration of NnrR protein

The analysis of haem-NnrR binding *in vitro* was performed using UV-Vis spectroscopy, a well-established technique for the characterisation of haem-bound proteins that offers high sensitivity and rapid data acquisition (Nienhaus and Nienhaus, 2005). This method exploits the distinct spectral properties of haem, which has characteristic absorption peaks in the visible region, allowing precise determination of haem binding and its redox state. To subtract background absorbance, a buffer sample is treated under identical conditions to the experimental samples and its spectrum is also recorded. The experiments in this study were run under anaerobic conditions, essentially following the protocol described by Giardina and coworkers (2008). Solutions at 10 μM and 20 μM of apoprotein NnrR (monomeric form) in reconstitution buffer (40 mM sodium phosphate, pH 7.5, 300 mM NaCl) were titrated individually with increasing amounts of 0.5 mM reduced hemin solution. Prior to the titration experiments, bovine hemin (Fluka) was dissolved in 0.1 mM NaOH and reduced with 3 mM sodium dithionite ($Na_2S_2O_4$) under anaerobic conditions. The hemin concentration in the protein solution increased after the addition of 22 aliquots of 2 μl. After each hemin addition, a full ultraviolet-visible (UV-Vis) spectrum (250 – 650 nm) was recorded in a spectrophotometer (WPA Biowave II).

The titration was carried out inside an anaerobic glove box under an inert N_2 atmosphere. All the solutions in rubber stoppered bottles were gassed with N_2 prior to introduction in the glove box (10 min for 25 ml volume or 45 min for larger volumes). The protein solution (1 ml) was gassed for only 3 min, to avoid excessive drying of the sample.

To determine the stoichiometry of NnrR:haem binding, the absorbance data at 427 nm were plotted against the haem concentration and a linear fit was performed using a double reciprocal plot. This fit allows the determination of the maximum OD_{427}, which corresponds to the point where the free haem concentration approaches zero, i.e., the maximum haem concentration bound to the protein, thus enabling the calculation of the stoichiometry of the haem-protein complex.

2.8. NnrR-haem reconstitution

The NnrR-haem reconstitution was performed following the methodology described by Giardina et al. (2008). Apo-NnrR protein was mixed with a 1:3 excess of hemin (NnrR:hemin). All solutions were gassed with N_2 to achieve anoxia prior to the experiment. After two hours of incubation of the mixture, the excess of hemin was removed by dialysis using a 3500 Da pore cassette (Slize-A-Lyzer, Thermo Fisher Scientific) against 1 L of reconstitution buffer (40 mM phosphate buffer, 300 mM NaCl, pH 7.5) overnight. After collecting the sample, a full UV-Vis spectrum of the protein bound to haem in its ferric form was performed. Then, the haem was reduced with an excess of 3 mM sodium dithionite and the full spectrum of NnrR:ferrous haem complex was collected. Finally, to determine the binding of NO to the NnrR:ferrous haem complex, NO gas solution (1.5 mM) was added in 1:1 ratio, and the full spectrum was determined again. UV-Vis spectra of haem-reconstituted NnrR were recorded on a UV1800 Shimadzu spectrophotometer, using a 1-cm quartz cuvette.

2.9. Biocomputing tools

De novo prediction of the NnrR protein structure was carried out with the ColabFold v1.5.5: AlphaFold2 using MMseqs2 (Mirdita et al., 2022), accessed on 14 November 2023. The Discovery Studio 2021 Client v21.1 software (BIOVIA, San Diego, Dassault Systèmes, 2021) was used for visualisation, analysis, and representation of the structures. The T-Coffee multiple sequence alignment server mode Expresso (https://tcoffee.crg.eu/apps/tcoffee/do:expresso, accessed on 26 June 2024) (Armougom et al., 2006; Di Tommaso et al., 2011) was used to generate an alignment of a selection of CRP/FNR proteins providing its sequences. Expresso server identified close homologues of the sequences within the Protein Data Bank (PDB) database through a BLAST, selecting the best hit based on a threshold of >30% identity over >50% of the query sequence. After assembling the library, the standard T-Coffee algorithm was used to generate the alignment. The resulting data for the phylogenetic tree was exported in a dnd file, which was then visualized using MEGA 5.1 software (https://www.megasoftware.net/).

2.10 Statistical analysis

Mean values are presented ± standard errors of at least three independent biological replicates, each performed in triplicate. Inferential statistics were performed using parametric analysis of variance (ANOVA) for unpaired data. A post-hoc Tukey HSD test at $P \leq 0.05$ was then performed using SPSS (v29) software. These analyses were undertaken assuming normal distribution and homoscedasticity of the raw data.

3. Results

3.1. NnrR activates norCBQD *gene expression in response to NO in a FixK$_2$-independent manner*

In *B. diazoefficiens*, NnrR is required for the maximal expression of *norCBQD* genes, which takes place under low-oxygen conditions in the presence of NO (Bueno et al., 2017). To analyse the effect of NO *per se* on *norCBQD* gene expression, the influence of addition of the NO scavenger cPTIO on the activity of a *norC-lacZ* transcriptional fusion and on NorC protein levels in cells cultured microaerobically and subsequently incubated with NO was investigated. As expected, *norC-lacZ* expression levels were basal in *B. diazoefficiens* wild type (WT) and *nnrR* and *fixK$_2$* mutants in the absence of NO (Fig. 1A). Addition of NO increased *norC-lacZ* expression in wild-type cells compared to that found in the absence of NO (463 ± 17.4 versus 50.4 ± 14.3; Fig. 1A), but not in the *nnrR* and *fixK$_2$* mutants, where β-galactosidase activity levels did not change upon addition of NO. Interestingly, the induction of *norC-lacZ* expression observed in the WT in the presence of NO was abolished when cPTIO was added to the growth medium, reducing it to near basal levels (87.6 ± 6) (Fig. 1A). In the same line, NorC protein levels in wild-type cells measured by *c*-type haem staining assays showed a similar behaviour to that observed for *norC-lacZ* expression (Fig. 1B). These results confirmed that NO is the signalling molecule that triggers maximal expression of *norCBQD* genes, and that signal perception is dependent on both FixK$_2$ and NnrR.

Since *nnrR* is a direct target of FixK$_2$, the question of whether or not the NnrR protein is able to activate *norCBQD* expression uncoupled from FixK$_2$ control was investigated. For this purpose, we determined β-galactosidase activity of the *norC-lacZ* fusion and NorC protein levels in a *fixK$_2$* mutant strain complemented *in trans* with the *nnrR* gene expressed from the constitutive *lacZ* promoter (Fig. 1A and C). In the complemented *fixK$_2$* strain, *norC-lacZ* expression was restored to wild-type levels when NO was added to the cultures (Fig. 1A). Indeed, the same expression profile was observed in an *nnrR* mutant complemented *in trans* with the gene expressed from its genuine FixK$_2$-dependent promoter, which was used as a positive control in our experiments (Fig. 1A). Furthermore, NorC protein levels in the complemented strains incubated in the presence of NO correlated with the expression profile of the *norC-lacZ* fusion (Fig. 1C). Taken together, these results indicate that NnrR induces *norCBQD* gene expression in response to NO independently of the FixK$_2$ protein.

3.2. Haem is the cofactor for B. diazoefficiens *NnrR*

In *B. diazoefficiens*, a mutant in *hemN₂* was unable to grow under denitrifying conditions and also showed reduced levels of NorC (Fischer et al., 2001). Therefore, our hypothesis was that if haem is also the cofactor for *B. diazoefficiens* NnrR to sense NO, then the mutation in *hemN₂* would affect NnrR activity, and therefore the expression of *norCBQD* genes. To verify this, the expression of the *norC-lacZ* fusion and NorC protein levels were monitored in the WT and a *hemN₂* mutant cultured under anaerobic conditions and incubated with or without 50 μM NO (Fig. 2). In the *hemN₂* mutant, β-galactosidase activity from the *norC-lacZ* fusion was 1.5 and 3.5-fold lower than that measured in the WT, both in the absence or in the presence of NO, respectively (Fig. 2A). The addition of hemin to *hemN₂* mutant cells incubated with NO increased *norC-lacZ* expression similar to WT levels of β-galactosidase activity. Analysis of NorC protein levels confirmed the *norC-lacZ* expression results, showing that the NorC profile was restored to wild-type levels in a *hemN₂* mutant upon addition of hemin (Fig. 2B). These data confirmed that haem synthesised by the pathway involving $HemN_2$ could be the cofactor for NnrR function *in vivo*.

The ability of NnrR to bind haem was also analysed spectroscopically *in vitro* (Fig. 3). For this purpose, titration experiments of recombinant NnrR apoprotein with hemin were performed under anaerobic conditions. Aliquots of reduced hemin were added to two independent NnrR protein solutions at a concentration of 10 μM and 20 μM (monomeric form). After each addition of hemin, a full UV-Vis spectrum (250-650 nm) was recorded (Fig. 3). Data analysis and normalisation of each spectrum, compared with the control titration on buffer, revealed three peaks; one at 280 nm, corresponding to the protein, and two prominent peaks at 427 nm and 560 nm, characteristic of the haem-bound NnrR complex. The peak at 427 nm represents the Soret band, a typical feature of haem proteins, and its position indicates the presence of a hexacoordinated low-spin ferrous haem. The appearance of this Soret band at 427 nm, together with the peak at 560 nm, is likely to result from ligand-to-metal charge transfer transitions within the haem protein complex. These spectral features strongly suggest that the haem iron in NnrR is coordinated by both axial ligands, probably a histidine residue from the protein and a potential exogenous ligand such as NO.

In order to calculate the stoichiometry of the NnrR:haem complex, absorbance values at 427 nm of each of the normalised spectra versus hemin concentration (Fig. S4) were analysed through a double reciprocal plot (Fig. 3, insert). The maximum OD_{427} values were 0.39 and 0.21 for the titrations of NnrR at 20 μM and 10 μM, respectively, which yielded hemin values of 22.8 μM (blue data) and 11.6 μM (pink data). These results suggest an NnrR:haem complex

stoichiometry of approximately 1 mol of haem per mol of NnrR monomer. The slight overestimation of the haem concentration compared to the actual protein concentration might be attributed to an underestimation of the initial haem concentration used in the titrations.

3.3. NnrR-ferrous haem complex is responsible for NO binding in vitro

To analyse whether the NnrR:haem complex can bind NO, the apo-NnrR was reconstituted with hemin under anaerobic conditions and a full UV-Vis absorption spectroscopic analysis performed. As shown in Fig. 4 (green line), the resulting holo-NnrR with the bound haem in its ferric form showed a prominent peak at 411 nm. Reduction of the bound haem to its ferrous form by the addition of an excess of the chemical reductant sodium dithionite, resulted in two peaks: one at 427 nm, and the other at 560 nm (Fig. 4, red line). The addition of NO gas to the NnrR-ferrous haem complex (1:1 stoichiometry) shifted the peak at 427 nm to 400 nm, which indicates binding of NO (Fig. 4, blue line). The results suggest that ferrous haem is the cofactor for NnrR to detect NO *in vitro*.

3.4. Histidine 11 is a relevant residue for NnrR function

The recorded spectra of *B. diazoefficiens* NnrR fitted to those of haem proteins with histidines as ligands, including NO-sensing regulators. Specifically, in *P. aeruginosa* DNR, H187 has been implicated in haem coordination, while H14 and H15 would play a role in protein-haem complex stabilisation (Giardina et al., 2008; Rinaldo et al., 2012; Cutruzzolá et al., 2014). In order to identify the specific residues of NnrR that are involved in haem binding, i.e., in the formation of the active holoprotein that triggers transcription activation of *norCBQD* genes, a *de novo* prediction of the quaternary structure of NnrR was performed using ColabFold v1.5.5: AlphaFold2 using MMseqs2 (Mirdita et al., 2022), accessed on 14 November 2023. The model showed that two histidine residues at the N-terminal domain of the protein, i.e., H11 and H56, are located in a hydrophobic pocket and they could act as haem ligands (Fig. 5A and B). Indeed, H56 is a fairly well conserved residue in other NnrR protein orthologues (Fig. 5C). Therefore, H11 and H56 residues were first replaced by alanine, individually or simultaneously, yielding H11A, H56A and H11A-H56A NnrR derivatives. The subsequent effects of each type of mutation were then analysed both *in vitro* and *in vivo*.

For the *in vitro* approach, the histidine mutant NnrR derivatives were overexpressed and purified as untagged proteins using the IMPACT system, following a protocol similar to that for the parental NnrR protein. After verifying the purity of each derivative (over 98%; Fig. S1), all proteins were reconstituted with hemin under anaerobic conditions as for the wild-type

protein, and the spectroscopic properties in the UV-Vis region were monitored (Fig. 6). The spectral properties of the single mutants H11A, and H56A were not different from those of the wild-type protein (comparison of Fig. 6 with Fig. 4), since the typical profiles for the ferrous (red line, peaks at 427 and 560 nm) and for the ferrous-NO binding (blue line, peak at 400 nm) proteins were still observed. However, in the case of H11A-H56A NnrR, a shoulder at 389 nm was detected in the ferrous form, indicating that a portion of free hemin is not bound to the protein derivative during reconstitution (Fig. 6, red line).

For the *in vivo* approach, *B. diazoefficiens* strains encoding NnrR protein derivatives with H11A, H56A and H11A-H56A mutations were constructed. Single or simultaneous alanine substitutions in H11 and H56 did not affect the ability of any of the mutant strains to grow under denitrifying conditions, as they exhibited the same behaviour as the WT (Fig. S5). However, the expression of a *norC-lacZ* fusion in the strains encoding H11A NnrR and H11-H56 NnrR was reduced to approximately half of the β-galactosidase activity determined in wild-type cells (Fig. 7A). This expression profile correlated with the reduction in NorC protein levels detected in both H11A and H11A-H56A NnrR encoding strains according to cytochrome *c* staining analysis (Fig. 7B). Similarly, a significant reduction (approximately 60%) in cNor enzyme activity, as determined by measuring NO consumption, was also observed in both the H11A NnrR and the H11A-H56A NnrR mutants (Fig. 7C). Since the behaviour of the H56A NnrR-encoding strain was similar to that of the WT in terms of *nor* expression and NorC levels and cNor activity (Fig. 7), we can conclude that H11 in NnrR is a relevant residue for NnrR function.

4. Discussion

Legumes are a rich source of protein and, due to their capacity to establish biological N_2-fixing symbiosis with rhizobia, they can safe huge amounts of environment polluting N fertilisers, which are important sources of NO and N_2O emissions, provoking a significant impact on climate change. However, rhizobia contribute to the production and consumption of NO and N_2O under both free-living and in symbiotic association with legumes (Torres et al., 2016; Sánchez and Minamisawa, 2019; Salas et al., 2021). These gases are intermediates of denitrification, being cNor encoded by the *norCBQD* genes, the key enzyme that reduces NO to the GHG N_2O. In this study, we have deepened in the regulatory mechanisms that control the expression of the *norCBQD* genes by the NnrR regulator in response to NO. This knowledge will be the basis for developing strategies to mitigate both NO and N_2O from legumes.

NnrR belongs to the CRP/FNR family of bacterial transcription factors, which differ in the signal they sense and therefore, have distinct molecular properties (Körner et al., 2003; Matsui et al., 2013). In the denitrification pathway, the reactions of NO_2^- reduction to NO and the subsequent detoxification through NO reduction to N_2O are often closely coupled and co-regulated. Within the CRP/FNR family, members of the DNR and NnrR clades are involved in the control of these tandem reactions in response to NO (Fig. 8). Whereas DNR-like proteins are mainly associated with γ-proteobacteria, and induce the expression of *cd*$_1$-type Nir-encoding genes, NnrR-like proteins are present in α-proteobacteria and activate genes that code for copper-containing Nir enzymes (Mesa et al., 2003; Matsui et al., 2013). Both DNR and NnrR clades remain poorly characterised despite their global importance in regulating the removal of NO as well as the synthesis of the GHG N_2O. Understanding the mechanism by which the synthesis and consumption of these gases occurs will be important in the context of a better knowledge of how to mitigate against their release in agricultural systems.

To date, biochemical studies have been limited to two NO-sensing CRP/FNR transcription factors: namely, DNR from *P. aeruginosa* (Giardina et al., 2008) and DnrF from *D. shibae* (Ebert et al., 2017), both of which belong to the DNR subgroup. However, the knowledge about how the members of the NnrR subgroup respond to NO remains unexplored. Here, to advance in the understanding of the molecular mechanism of members of the NnrR clade to perceive NO, we performed a series of *in vivo* and *in vitro* experiments for the characterisation of the NnrR regulator of the soybean endosymbiont *B. diazoefficiens*.

As for other denitrifiers including rhizobial species, NO is the signalling molecule needed for maximal induction of the *B. diazoefficiens norCBQD* gene cluster (Bueno et al., 2017). This requirement was confirmed in the present work (Fig. 1). Specifically, the addition of an NO scavenger significantly reduced the expression of a *norC-lacZ* fusion and NorC protein levels in the WT cultured microaerobically and incubated in the presence of NO. These results also confirmed that NO-mediated induction of the *norCBQD* genes is dependent on both $FixK_2$ and NnrR, as reported elsewhere (Bueno et al., 2017). However, since *nnrR* is a direct target for the superimposed $FixK_2$ protein in the hierarchical FixLJ-$FixK_2$-NnrR regulatory cascade (Jimenez-Leiva et al., 2019), we could not dissect which regulator is responsible for the maximal activation of *norCBQD*. The complementation *in trans* of a *fixK*$_2$ mutant strain with a plasmid constitutively expressing the *nnrR* gene, restored *norC-lacZ* expression and NorC protein levels to wild-type levels in response to NO (Fig. 1). Thus, NnrR is the direct activator for *norCBQD* genes expression in a manner that is independent of $FixK_2$. These findings are

consistent with those reported by Bueno and coworkers (2017), where recombinant NnrR protein interacted with the promoter of *norCBQD* genes *in vitro*. Therefore, the reduced expression of *norCBQD* genes in the *fixK*$_2$ mutant is an indirect effect due to the dependence of *nnrR* transcriptional activation on FixK$_2$.

In other rhizobial species such as *Rhizobium etli* and *Sinorhizobium meliloti*, NnrR-type proteins are also involved in NO-mediated induction of *norCBQD* (Meilhoc et al., 2010; Cabrera et al., 2011; Gómez-Hernández et al., 2011). In *R. etli*, the control by NnrR is integrated into a microaerobic-responsive alternative cascade and depends on FixKf, a FixK-like orthologue. However, in *S. meliloti*, NnrR integrates the NO signal for *norCBQD* activation uncoupled from FixK (Meilhoc et al., 2010; Cabrera et al., 2011; Zamorano-Sánchez and Girard, 2015).

NO perception in both DNR from *P. aeruginosa* (Giardina et al., 2008) and DnrF from *D. shibae* (Ebert et al., 2017) occurs via ferrous haem as a cofactor. To explore whether this is the case for *B. diazoefficiens* NnrR, expression of a *norC-lacZ* fusion and analysis of NorC protein levels were determined in a strain lacking *hemN*$_2$, a gene encoding the HemN$_2$ protein which is involved in haem biosynthesis under denitrifying conditions (Fischer et al., 2001). Both *norCBQD* expression and NorC protein levels were reduced in the *hemN*$_2$ mutant cultured anaerobically and incubated in the presence of NO and restored to near wild-type levels when hemin was added to the cultures (Fig. 2). This suggests a role for HemN$_2$ in the production of haem required for NO sensing and NnrR activity *in vivo*. Indeed, Fischer et al. (2001) previously showed that the impairment of the *hemN*$_2$ mutant to grow under denitrifying conditions can be complemented by exogenous hemin, so it can enter to the cells, probably, by a haem transport system (Nienaber et al., 2001). Furthermore, *hemN*$_2$ belongs to the FixK$_2$ regulon under microaerobic conditions and indeed, it is a direct target for this transcription factor (Mesa et al., 2005; Mesa et al., 2008). The expression of *hemN*$_2$ is also downregulated in an *nnrR* mutant cultured under denitrifying conditions (Jiménez-Leiva et al., 2019). Thus, a scenario can be proposed in which both *hemN*$_2$ and *nnrR* are initially induced by FixK$_2$ under microaerobic conditions and that, under denitrifying conditions, the holo-NnrR protein boosts *hemN*$_2$ expression, thereby controlling its own activity.

These results added an additional role for haem to those that have been described so far in rhizobia, such as NO detoxification, as a cofactor of haemoglobins (Salas et al., 2021). In particular, in *S. meliloti*, a flavohaemoglobin encoded by *hmp* plays a role in NO resistance in free-living cells (Meilhoc et al., 2010) and in symbiosis with *Medicago truncatula* (Cam et al.,

2012). In *B. diazoefficiens*, a single-domain haemoglobin (designated Bjgb) is also involved in NO detoxification (Cabrera et al., 2016) as well as in the modulation of NO levels in soybean nodules (Salas et al., 2020). Furthermore, haem is also the cofactor of the cytochrome *c* oxidase cbb_3 which is essential to support microaerobic respiration for nitrogen fixation (Bueno et al., 2012; Salas et al., 2021).

That haem is the cofactor for *B. diazoefficiens* NnrR was also confirmed *in vitro*. Titration assays showed that NnrR binds hemin with a 1:1 stoichiometry (NnrR monomer:haem) (Fig. 3). Furthermore, the full UV-Visible spectra of haem-reconstituted NnrR showed the typical spectroscopic properties of a haem-protein complex able to react with NO: (i) the oxidised (ferric) form (peak at 411 nm), (ii) the reduced (six-coordinated ferrous) form (peaks at 427 nm and 560 nm), and the ferrous form bound to NO (peak at 400 nm) (Fig. 4). These spectroscopic features are similar to those previously observed for both *P. aeruginosa* DNR and *D. shibae* DnrF (Ebert et al., 2017; Giardina et al., 2008).

Within the CRP/FNR family members, alternative NO sensing mechanisms have been described (Körner et al., 2003; Spiro, 2007; Matsui et al., 2013; Tinajero-Trejo and Shepherd, 2013). This is the case of *Escherichia coli* FNR, which in addition to being an archetype that responds to low oxygen conditions, it is also capable of sensing NO. In particular, FNR is inactivated by NO under anaerobic conditions by nitrosylation of the oxygen-sensitive $[4Fe\text{-}4S]^{2+}$ cluster, yielding a mixture of monomeric and dimeric dinitrosyl-iron-cysteine species (Cruz-Ramos et al., 2002; Crack et al., 2008). NssR from *Campylobacter jejuni* (Elvers et al., 2005) constitutes another example of a CRP/FNR-type regulator that mediates the NO response by an alternative mechanism. Although not proven, it has been proposed that nitrosative stress conditions trigger nitrosylation of the single cysteine or nitration of one of the several tyrosine residues present in the structure of NssR (Smith et al., 2011).

P. aeruginosa DNR is an extremely flexible protein that adopts several conformational changes from the inactive (OFF) (Fig. 9) to the active (ON) conformation (Rinaldo et al., 2012). This reorganisation leads to the building of a hydrophobic pocket for haem binding where residues H14, H15 and H187 are located. While either of the two first residues are involved in haem-binding stabilisation, H187 is directly involved in iron coordination (Cutruzzolá et al., 2014; Rinaldo et al., 2012). As yet, no experimentally-derived structure of a member of the NnrR clade has been solved. This makes it difficult to predict the residues of *B. diazoefficiens* NnrR, which *a priori*, might be involved in haem binding. However, *de novo* prediction using ColabFold showed a model of *B. diazoefficiens* NnrR as a homodimer, whose monomers

595 interact with each other through an α-helix (Fig. 5A). This modelling also allowed us to infer a
596 hydrophobic cavity in the N-terminal region of NnrR that can act as a potential haem-binding
597 pocket (Fig. 5B). Within this pocket, two histidine residues, H11 and H56 could be important
598 for the functionality of NnrR since histidines are more typical haem-binding residues (Li et al.,
599 2011). Furthermore, H56 is a conserved residue in other NnrR orthologues (Fig. 5C). Although
600 single alanine substitutions of H11 and H56 in NnrR had no effect on the ability of NnrR to
601 bind haem (Fig. 6), the spectroscopic properties of the H11A-H56A NnrR protein derivative
602 indicated that the ferrous haem-protein complex appeared to be more unstable, as a shoulder
603 was detected at 389 nm in the ferrous form (Fig. 6). However, in both the H11A NnrR and
604 H11A-H56A NnrR encoding strains, the expression of *norCBQD* in response to NO was
605 reduced to half of wild-type levels. A similar reduction in NorC levels and cNor activity was
606 also observed (Fig. 7). Our hypothesis is that, *in vitro*, under hemin excess conditions, the
607 phenotype could only be observed in the double H11A-H56A NnrR mutant variant, whereas *in*
608 *vivo*, under physiological levels of hemin, the phenotype is already detected in the single H11
609 NnrR mutant. Thus, both H11 and H56 residues contribute to the stability of the haem-loaded
610 NnrR protein, whereas H11 seems to be an important residue for the optimal activity of this
611 regulator.

612 Carbon monoxide (CO)-sensing regulators belonging to the CRP/FNR family have evolved
613 together with the NnrR clade from an ancestral FNR-type protein (Matsui et al., 2013; Fig. 8).
614 These CO sensors also bind haem as a cofactor through a central (proximal) histidine residue
615 of one monomer and a non-specifically defined N-terminal (distal) residue of the other
616 monomer. Whereas in *Rhodospirillum rubrum* CooA these residues correspond to H77 and P2
617 (Lanzilotta et al., 2000; Fig. 9), H82 and M1 are the equivalent amino acids in
618 *Carboxydothermus hydrogenoformans* (Borjigin et al., 2006) (Fig. 9). So, stabilisation of haem
619 might be a major role of the N terminus of CooA. The comparison of the predicted *B.*
620 *diazoefficiens* NnrR structure with that of CooA of *R. rubrum* and of *C. hydrogenoformans*
621 revealed that the equivalent residue to the proximal histidine residue in these proteins would
622 correspond to M86 or Y93 in NnrR (Fig. 9). Then, the N-terminal H11 residue in *B.*
623 *diazoefficiens* NnrR would play a role in the stabilisation of the protein-haem complex, while
624 either M86 or Y93 might bind directly to this cofactor. This hypothesis sounds plausible, since
625 alternative residues such as methionine or tyrosine have been proposed as typical ligands for
626 haem binding (Li et al., 2011). Thus, a functional mutagenesis of M86 and Y93 in NnrR will

be an interesting approach for future investigations, which we believe is beyond the scope of this work.

Taken together, based on the results with the NnrR of B. *diazoefficiens*, we provide strong evidence supporting that the NnrR clade binds haem as a cofactor to sense NO. These findings also constitute the first insights into the molecular mechanism of an NnrR-type protein and further advances into the biochemical and cellular functions of a rhizobial NO-sensing regulator. By gaining a comprehensive understanding of how the NnrR protein functions, we can strategically manipulate microbial processes, such as denitrification, with the aim of advancing biotechnological and environmental applications. This knowledge can serve as a basis for developing strategies to mitigate the emissions of the potent GHG N_2O triggered by rhizobial species from agricultural soils.

CRediT authorship contribution statement

Andrea Jiménez-Leiva: Data curation; Formal analysis; Investigation; Methodology; Software; Validation; Visualization; Writing - original draft; Writing - review & editing. **Juan J. Cabrera:** Data curation; Investigation; Methodology; Software; Validation; Visualization; Writing - review & editing. **María J. Torres:** Investigation; Methodology; Writing - review & editing. **David J. Richardson:** Resources; Writing - review & editing. **Eulogio J. Bedmar:** Funding acquisition; Resources; Writing - review & editing**. Andrew J. Gates:** Data curation; Formal analysis**;** Funding acquisition; Resources; Writing - review & editing. **María J. Delgado:** Conceptualization; Funding acquisition; Project administration, Resources; Supervision; Writing - original draft; and Writing - review & editing. **Socorro Mesa:** Conceptualization; Data curation; Formal analysis; Funding acquisition; Project administration, Resources; Supervision; Writing - original draft; Writing - review & editing.

Declaration of Competing Interest

Authors declare that they have no competing interest in the present work.

Data Availability

Data will be available on request.

Acknowledgements

This work was supported by grant PID2020-114330GB-I00 funded by MCIN/AEI/10.13039/501100011033 to S. Mesa. Grants AGL2015-63651-P to S. Mesa, and AGL2017-85676-R and PID2021-124007OB-I00 to M.J. Delgado, both funded by MCIN/AEI/10.13039/501100011033 and "ERDF A way of making Europe" are also acknowledged. E.J. Bedmar, M.J. Delgado and S. Mesa thank Junta de Andalucía, Spain (grants P12-AGR-1968, and P18-RT-1401 and continuous support to Group BIO-275). A. Jiménez-Leiva was financed by grants P12-AGR-1968 and P18-RT-1401 during her PhD Thesis and postdoctoral period. J.J. Cabrera and M.J. Torres were supported by contracts funded by grants AGL2015-63651-P, and AGL2017-85676-R, respectively. Germán Tortosa and Alba Hidalgo-García (Estación Experimental del Zaidín, CSIC, Granada, Spain) are acknowledged for their excellent technical support.

Appendix A. Supporting information

Supplementary data associated with this article can be found in the online version at …

References

Armougom F., Moretti S., Poirot O., Audic S., Dumas P., Schaeli B., Keduas V., Notredame C., 2006. Expresso: automatic incorporation of structural information in multiple sequence alignments using 3D-Coffee. Nucleic Acids Res. 1:34.

Bedmar, E.J., Robles, E.F., Delgado, M.J., 2005. The complete denitrification pathway of the symbiotic, nitrogen-fixing bacterium *Bradyrhizobium japonicum*. Biochem. Soc. Trans. 33:141-144.

Borjigin, M., Li, H., Lanz, N.D., Kerby, R.L., Roberts, G.P., Poulos, T.L., 2007. Structure-based hypothesis on the activation of the CO-sensing transcription factor CooA. Acta. Crystallogr. D. Biol. Crystallogr. 63:282-287.

Browning, D.F., Busby, S.J., 2004. The regulation of bacterial transcription initiation. Nat. Rev. Microbiol. 2:57-65.

Bueno, E., Mesa, S., Bedmar, E.J., Richardson, D.J., Delgado, M.J., 2012. Bacterial adaptation of respiration from oxic to microoxic and anoxic conditions: redox control. Antioxid. Redox Signal. 16:819-852.

Bueno, E., Robles, E.F., Torres, M.J., Krell, T., Bedmar, E.J., Delgado, M.J., Mesa, S., 2017. Disparate response to microoxia and nitrogen oxides of the *Bradyrhizobium japonicum napEDABC, nirK* and *norCBQD* denitrification genes. Nitric Oxide. 68:137-149.

Cabrera, J.J., Jiménez-Leiva, A., Tomás-Gallardo, L., Parejo, S., Casado, S., Torres, M.J., Bedmar, E.J., Delgado, M.J., Mesa, S., 2021. Dissection of $FixK_2$ protein-DNA interaction unveils new insights into *Bradyrhizobium diazoefficiens* lifestyles control. Environ. Microbiol. 23:6194-6209.

Cabrera, J.J., Salas, A., Torres, M.J., Bedmar, E.J., Richardson, D.J., Gates, A.J., Delgado, M.J., 2016. An integrated biochemical system for nitrate assimilation and nitric oxide detoxification in *Bradyrhizobium japonicum*. Biochem. J. 473:297-309.

694 Cabrera, J.J., Sánchez, C., Gates, A.J., Bedmar, E.J., Mesa, S., Richardson, D.J., Delgado, M.J.,
695 2011. The nitric oxide response in plant-associated endosymbiotic bacteria. Biochem.
696 Soc. Trans. 39:1880-1885.

697 Cam, Y., Pierre O., Boncompagni, E., Hérouart, D., Meilhoc, E., Bruand, C., 2012. Nitric oxide
698 (NO): a key player in the senescence of *Medicago truncatula* root nodules. New. Phytol.
699 196:548-560.

700 Castiglione, N., Rinaldo, S., Giardina, G., Cutruzzolá, F., 2009. The transcription factor DNR
701 from *Pseudomonas aeruginosa* specifically requires nitric oxide and haem for the
702 activation of a target promoter in *Escherichia coli*. Microbiol. 155:2838-2844.

703 Crack, J.C., Le Brun, N.E., Thomson, A.J., Green, J., Jervis. A.J., 2008. Reactions of nitric
704 oxide and oxygen with the regulator of fumarate and nitrate reduction, a global
705 transcriptional regulator, during anaerobic growth of *Escherichia coli*. Methods Enzymol.
706 437:191-209.

707 Cruz-Ramos, H., Crack, J., Wu, G., Hughes, M.N., Scott, C., Thomson, A.J., Green, J., Poole,
708 R.K., 2002. NO sensing by FNR: regulation of the *Escherichia coli* NO-detoxifying
709 flavohaemoglobin, Hmp. EMBO J. 21:3235-3244.

710 Cutruzzolá, F., Arcovito, A., Giardina, G., della Longa, S., D'Angelo, P., Rinaldo, S., 2014.
711 Distal-proximal crosstalk in the heme binding pocket of the NO sensor DNR. Biometals.
712 27:763-773.

713 Daniel, R.M., Appleby, C.A., 1972. Anaerobic-nitrate, symbiotic and aerobic growth of
714 *Rhizobium japonicum*: effects on cytochrome P450, other haemoproteins, nitrate and
715 nitrite reductases. Biochim. Biophys. Acta. 275:347-354.

716 Di Tommaso, P., Moretti, S., Xenarios, I., Orobitg, M., Montanyola, A., Chang, J.M., Taly,
717 J.F., Notredame, C, 2011. T-Coffee: a web server for the multiple sequence alignment of
718 protein and RNA sequences using structural information and homology extension.
719 Nucleic Acids Res. 39:13-17.

720 Dufour, Y.S., Kiley, P.J., Donohue, T.J., 2010. Reconstruction of the core and extended
721 regulons of global transcription factors. PLoS Genet. 6:e1001027.

722 Ebert, M., Schweyen, P., Broring, M., Laass, S., Hartig, E., Jahn, D., 2017. Heme and nitric
723 oxide binding by the transcriptional regulator DnrF from the marine bacterium
724 *Dinoroseobacter shibae* increases *napD* promoter affinity. J. Biol. Chem. 292:15468-
725 15480.

726 Elvers, K.T., Turner, S.M., Wainwright, L.M., Marsden, G., Hinds, J., Cole, J.A., Poole, R.K.,
727 Penn, C.W., Park, S.F., 2005. NssR, a member of the Crp-Fnr superfamily from
728 *Campylobacter jejuni*, regulates a nitrosative stress-responsive regulon that includes both
729 a single-domain and a truncated haemoglobin. Mol. Microbiol. 57:735-750.

730 Farhana, A., Saini, V., Kumar, A., Lancaster, J.R., Jr., Steyn, A.J., 2012. Environmental heme-
731 based sensor proteins: implications for understanding bacterial pathogenesis. Antioxid.
732 Redox Signal. 17:1232-1245.

733 Fernández, N., Cabrera, J.J., Salazar, S., Parejo, S., Rodríguez, M.C., Lindemann, A., Bonnet,
734 M., Hennecke, H., Bedmar, E.J., Mesa, S., 2016. Molecular determinants of negative
735 regulation of the *Bradyrhizobium diazoefficiens* transcription factor $FixK_2$. In: González-
736 Andrés F., James E. (eds.), Biological nitrogen fixation and beneficial plant-microbe
737 interaction. Cham: Springer International Publishing; pp. 57-72.

738 Fischer, H.M., Velasco, L., Delgado, M.J., Bedmar, E.J., Schären, S., Zingg, D., Göttfert, M.,
739 Hennecke, H., 2001. One of two *hemN* genes in *Bradyrhizobium japonicum* is functional
740 during anaerobic growth and in symbiosis. J. Bacteriol. 183:1300-1311.

741 Fonseca, B.M., Paquete, C.M., Louro, R.O., 2014. Molecular mechanisms of heme based
742 sensors from sediment organisms capable of extracellular electron transfer. J. Inorg.
743 Biochem. 133:104-109.

744 Giardina, G., Rinaldo, S., Johnson, K.A., Di Matteo, A., Brunori, M., Cutruzzolá, F., 2008. NO
745 sensing in *Pseudomonas aeruginosa*: structure of the transcriptional regulator DNR.
746 J. Mol. Biol. 378:1002-1015.

747 Giardina, G., Rinaldo, S., Castiglione, N., Caruso, M., Cutruzzolá, F., 2009. A dramatic
748 conformational rearrangement is necessary for the activation of DNR from *Pseudomonas*
749 *aeruginosa*. Crystal structure of wild-type DNR. Proteins. 77:174-180.

750 Gómez-Hernández N, Reyes-González A, Sánchez C, Mora Y, Delgado M.J., Girard L., 2011.
751 Regulation and symbiotic role of *nirK* and *norC* expression in *Rhizobium etli*. Mol. Plant-
752 Microbe Interact. 24:233-245.

753 Jiménez-Leiva, A., Cabrera, J.J., Bueno, E., Torres, M.J., Salazar, S., Bedmar, E.J., Delgado,
754 M.J., Mesa, S., 2019. Expanding the regulon of the *Bradyrhizobium diazoefficiens* NnrR
755 transcription factor: new insights into the denitrification pathway. Front. Microbiol.
756 10:1926.

757 Körner, H., Sofia, H.J., Zumft, W.G., 2003. Phylogeny of the bacterial superfamily of Crp-Fnr
758 transcription regulators: exploiting the metabolic spectrum by controlling alternative gene
759 programs. FEMS Microbiol. Rev. 27:559-592.

760 Lanzilotta, W.N., Schuller, D.J., Thorsteinsson, M.V., Kerby, R.L., Roberts, G.P., Poulos, T.L.,
761 2000. Structure of the CO sensing transcription activator CooA. Nat. Struct. Biol. 7:876-
762 880.

763 Li, T., Bonkovsky, H.L., Guo, J.T., 2011. Structural analysis of heme proteins: implications for
764 design and prediction. BMC Struct. Biol. 11:13.

765 Matsui, M., Tomita, M., Kanai, A., 2013. Comprehensive computational analysis of bacterial
766 CRP/FNR superfamily and its target motifs reveals stepwise evolution of transcriptional
767 networks. Genome Biol. Evol. 5:267-282.

768 Meilhoc, E., Cam Y., Skapski, A, Bruand, C., 2010. The response to nitric oxide of the nitrogen-
769 fixing symbiont *Sinorhizobium meliloti*. Mol. Plant-Microbe. Interact. 23:748-759.

770 Mesa, S., Bedmar, E.J., Chanfon, A., Hennecke, H., Fischer, H.M., 2003. *Bradyrhizobium*
771 *japonicum* NnrR, a denitrification regulator, expands the FixLJ-$FixK_2$ regulatory cascade.
772 J. Bacteriol. 185:3978-3982.

773 Mesa S., Ucurum Z., Hennecke H., Fischer H.M., 2005. Transcription activation *in vitro* by the
774 *Bradyrhizobium japonicum* regulatory protein $FixK_2$. J. Bacteriol. 187:3329-3338.

775 Mesa, S., Hauser, F., Friberg, M., Malaguti, E., Fischer, H.M., Hennecke, H., 2008.
776 Comprehensive assessment of the regulons controlled by the FixLJ-$FixK_2$-$FixK_1$ cascade
777 in *Bradyrhizobium japonicum*. J. Bacteriol. 190:6568-6579.

778 Miller, J.H., 1972. Experiments in Molecular Genetics, Cold Spring Harbor Laboratory, New
779 York.

780 Mirdita, M., Schütze, K., Moriwaki, Y., Heo, L., Ovchinnikov, S., Steinegger, M., 2022.
781 ColabFold: making protein folding accessible to all. Nat. Methods. 19:679-682.

Nienaber, A., Hennecke, H., Fischer, H.M., 2001. Discovery of a haem uptake system in the soil bacterium *Bradyrhizobium japonicum*. Mol. Microbiol. 41:787-800.

Nienhaus, K., Nienhaus, G.U., 2005. Probing heme protein-ligand interactions by UV/visible absorption spectroscopy. Methods. Mol. Biol. 305:215-242.

Regensburger, B., Hennecke, H., 1983. RNA polymerase from *Rhizobium japonicum*. Arch. Microbiol. 135:103-109.

Richardson, D., 2011. Redox complexes of the nitrogen cycle. In: Moir, J.W.B. (ed.), Nitrogen cycling in bacteria: molecular analysis. Norfolk: Caister Academic Press; pp. 23-39.

Rinaldo, S., Castiglione, N., Giardina, G., Caruso, M., Arcovito, A., Longa, S.D., D'Angelo, P., Cutruzzolá, F., 2012. Unusual heme binding properties of the dissimilative nitrate respiration regulator, a bacterial nitric oxide sensor. Antioxid. Redox Signal. 17:1178-1189.

Salas, A., Cabrera, J.J., Jiménez-Leiva, A., Mesa, S., Bedmar, E.J., Richardson, D.J., Gates, A.J., Delgado, M.J., 2021. Bacterial nitric oxide metabolism: Recent insights in rhizobia. Adv. Microb. Physiol. 78:259-315.

Salas, A., Tortosa, G., Hidalgo-García, A., Delgado, A., Bedmar, E.J., Richardson, D.J., Gates, A.J., Delgado, M.J., 2019. The hemoglobin Bjgb from *Bradyrhizobium diazoefficiens* controls NO homeostasis in soybean nodules to protect symbiotic nitrogen fixation. Front. Microbiol. 10:2915

Sánchez, C., Minamisawa, K., 2019. Nitrogen cycling in soybean rhizosphere: sources and sinks of nitrous oxide (N_2O). Front. Microbiol. 10:1943.

Smith, H.K., Shepherd, M., Monk, C., Green, J., Poole, R.K., 2011. The NO-responsive hemoglobins of *Campylobacter jejuni*: concerted responses of two globins to NO and evidence *in vitro* for globin regulation by the transcription factor NssR. Nitric Oxide. 25:234-241.

Spiro S., 2007. Regulators of bacterial responses to nitric oxide. FEMS Microbiol. Rev. 31:193-211.

Spiro, S., 2011. Nitric oxide metabolism: physiology and regulatory mechanisms. In: Moir J.W.B. (ed.), Nitrogen cycling in bacteria: molecular analysis. Norfolk: Caister Academic Press; pp. 177-196.

Stern, A.M., Zhu, J., 2014. An introduction to nitric oxide sensing and response in bacteria. Adv. Appl. Microbiol. 87:187-220.

Tinajero-Trejo, M., Shepherd, M., 2013. The globins of *Campylobacter jejuni*. Adv. Microb. Physiol. 63:97-145.

Toledo, J.C., Jr. Augusto, O., 2012. Connecting the chemical and biological properties of nitric oxide. Chem. Res. Toxicol. 25:975-89.

Tomás-Gallardo, L., Cabrera, J.J., Mesa, S., 2024. Surface plasmon resonance as a tool to elucidate the molecular determinants of key transcriptional regulators controlling rhizobial lifestyles. Methods Mol. Biol. 2751:145-163.

Torres, M.J., Simon, J., Rowley, G., Bedmar, E.J., Richardson, D.J., Gates, A.J., Delgado, M.J., 2016. Nitrous oxide metabolism in nitrate-reducing bacteria: Physiology and regulatory mechanisms. Adv. Microb. Physiol. 68:353-432.

824 Torres, M.J., Bueno, E., Jiménez-Leiva, A., Cabrera, J.J., Bedmar, E.J., Mesa, S., Delgado,
825 M.J., 2017. $FixK_2$ is the main transcriptional activator of *Bradyrhizobium diazoefficiens*
826 *nosRZDYFLX* genes in response to low oxygen. Front. Microbiol. 8:1621.

827 van Spanning, R.J.M., Richardson, D.J., Ferguson, S.J., 2007. Introduction to the biochemistry
828 and molecular biology of denitrification, In: Bothe, H., Ferguson, S.J., Newton, W. E.
829 (eds.), Biology of the nitrogen cycle. Amsterdam: Elsevier; pp. 3-20.

830 Zamorano-Sánchez D., Girard L., 2015. FNR-like proteins in rhizobia: past and future. In: De
831 Bruijn, F.J. (ed.), Biological nitrogen fixation. Hoboken, New Jersey: John Wiley & Sons,
832 Inc; pp. 155-166.

833 Zumft, W.G., 1997. Cell biology and molecular basis of denitrification. Microbiol. Mol. Biol.
834 Rev. 61:533-616.

835

Figure captions

Fig. 1. NnrR activates *norCBQD* genes expression in response to NO uncoupled from $FixK_2$ control. β-galactosidase activity of a *norC-lacZ* fusion (A) and *c*-type haem staining (B and C) were determined in a battery of *B. diazoefficiens* strains cultured in YEM medium under microaerobic conditions (2% O_2) for 24 h, in the presence or the absence of 50 μM NO, added to the cultures 5 h before of the assays. 1 mM of the NO-scavenger cPTIO was added to some of the cultures. Values ± standard errors in A are the means of a representative experiment assayed in quadruplicate. At least three independent biological replicates were performed. Different capital or lower-case letters indicate that values are statistically different according to a post-hoc Tukey HSD test at $p \leq 0.05$. Capital letters show comparisons between strains while lower case letters indicate comparisons between the three conditions assayed: without NO, with NO and with NO and cPTIO. Full scan of the Coomassie blue-stained SDS-PAGE gel after protein transfer for haem-staining (B and C) are shown in Fig. S2.

Fig. 2. Induction of *norCBQD* genes is dependent on $hemN_2$. β-galactosidase activity of a *norC-lacZ* fusion (A) and *c*-type haem staining (B) were determined in *B. diazoefficiens* WT and a $hemN_2$ mutant in the presence and the absence of NO. Hemin (15 μg/ml) was added to a set of cultures of the $hemN_2$ mutant. Cells were cultured for 24 h under anaerobic conditions in YEM medium and 50 μM NO was added 5 h before activity determination, when indicated. Values ± standard errors in A are the means of a representative experiment assayed in triplicates. At least three independent biological replicates were performed. Different capital or lower case letters indicate that values are statistically different according to a post-hoc Tukey HSD test at $p \leq 0.05$. Capital letters show comparisons between strains while lower case letters indicate comparisons between conditions (absence or presence of NO). Full scan of the Coomassie blue-stained SDS-PAGE gel after protein transfer for haem-staining (B) is shown in Fig. S3.

Fig. 3. NnrR binds haem *in vitro*. Spectral changes of 20 μM NnrR protein (monomer) upon titration with increasing concentration of reduced hemin, ranging from 0 to 40 μM, under anaerobic conditions. The data were normalised to the wavelengths of 281 nm and 650 nm. The insert panel shows the double reciprocal plot of the absorbance values at 427 nm versus hemin concentration, obtained from each of the NnrR titrations at 10 μM (pink) and 20 μM (blue). The corresponding equations of the lines and their R^2 values are also presented. A minimum of three independent experiments were performed.

Fig. 4. Spectroscopic properties and reactivity of holo-NnrR with NO. Full UV-visible absorption spectra (250-650 nm) of the haem-reconstituted NnrR protein in three oxidation states: ferric (green line), ferrous (red line), and ferrous bound to nitric oxide (NO) (blue line) were recorded under anaerobic conditions. Ferric holo-NnrR was obtained by addition of an excess of hemin (1:3) which was reduced by addition of 3 mM of sodium dithionite yielding the ferrous form. Then, NO gas solution (1.5 mM) was added in 1:1 ratio resulting in the ferrous NO-bound complex. At least three independent experiments were performed.

Fig. 5. Structure of *B. diazoefficiens* NnrR and its hydrophobic pocket. (A) Ribbon representation of the predicted structure of NnrR dimer generated by ColabFold v1.5.5: AlphaFold2 using MMseqs2 (Mirdita et al., 2022), accessed on 14 November 2023. Each monomer is coloured differently (pink and fuchsia). The H11 and H56 residues are highlighted in green. (B) Hydrophobic surface representation of NnrR, highlighting a putative hydrophobic pocket (indicated with a red circle). (C) Multiple sequence alignment of NnrR from *B. diazoefficiens* (accession no. BAC52349) with homologues from *Sinorhizobium meliloti* 2011 (accession no. AGG70365), *Rhodopseudomonas palustris* CGA009 (accession no. AVT83001), *Neorhizobium galegae* bv. orientalis (accession no. CDZ63311), and *Pseudomonas* sp. G-179 (accession no. AAB96771). The alignment was generated using Clustal Omega (https://www.ebi.ac.uk/jdispatcher/, accessed on 20 May 2021). The H11 and H56 residues are marked with a green square.

Fig. 6. Spectral properties of a series of NnrR derivatives. Full UV-Visible spectra (250-650 nm) of holo-NnrR protein derivatives in their ferrous form (red line) and ferrous form bound to NO (blue line) were recorded under anaerobic conditions. H11A, left; H56A, middle; H11A-H56A, right. The profile of the ferrous form of the double the H11-H56 NnrR mutant protein showed a shoulder at 389 nm (marked with an arrow), indicating a lower stability of the protein-DNA complex so that a portion of the free hemin is not bound to this protein variant. At least three independent experiments were performed.

Fig. 7. The H11 residue is important for NnrR function *in vivo*. β-galactosidase activity of a *norC-lacZ* fusion (A), *c*-type haem staining (B) and cNor activity (C) determined in different *B. diazoefficiens* strains. Parental (WT), and H11A, H56A and H11A-H56A *nnrR* point mutation strains were cultured in YEMN medium under microoxic conditions (2% O_2) for 24 h. Values in (A) and (C) are means ± standard errors from a representative experiment performed in quadruplicate. Different lower case letters indicate that values are statistically

different according to a post-hoc Tukey HSD test at $p \leq 0.05$. Full scan of the Coomassie blue-stained SDS-PAGE gel after protein transfer for haem-staining (B) is shown in Fig. S6.

Fig. 8. Phylogenetic tree of a selection of CRP/FNR-like transcriptional regulatory proteins. Amino acid sequences were aligned using structural information with the T-COFFEE Expresso server (https://tcoffee.crg.eu/apps/tcoffee/do:expresso; accessed on 11 March 2024), and phylogenetic analyses were visualised with MEGA 5.1 software (https://www.megasoftware.net/). The different clades within the CRP/FNR family are shown at the right. The scale bar represents a distance of 0.02 substitutions per position. Accession numbers of individual protein sequences are indicated in parentheses beside the corresponding name of the following proteins: *P. aeruginosa* DNR; *D. shibae* Dnr; *R. rubrum* CooA; *C. hydrogenoformans* CooA; *B. diazoefficiens* NnrR; *R. palustris* NnrR; *S. meliloti* 2011 NnrR; *S. meliloti* 1021 NnrR; *Rhizobium phaseoli* Ch24-10 NnrR; *R. etli* CNF42 NnrR; *Pseudomonas* sp. G-179 NnrR; *N. galegae* bv. orientalis NnrR; *Cereibacter sphaeroides* (*Rhodobacter sphaeroides* 2.4.1) NnrR.

Fig. 9. Haem binding pocket and key residues in a selection of CO or NO sensing CRP-FNR transcription factors. Both CooA of *C. hydrogenoformans* (PDB: 2FMY) and of *R. rumbrum* (PDB: 4K8F) were solved as dimeric holo-proteins (haem cofactor in red) being H82 and H77 of one monomer the axial haem-binding residues, and M1 and P2 of the other monomer the haem stabilising residues. Shown are the positions of residues H14, H15 and H187 in *P. aeruginosa* DNR solved protein (PDB:3DKW) and H11, H56, M86, and Y96 in *B. diazoefficiens* NnrR predicted structure (ColabFold), which might have a role in the interaction with haem as cofactor. For a matter of simplicity, the structure of one of the monomers is shown transparent.

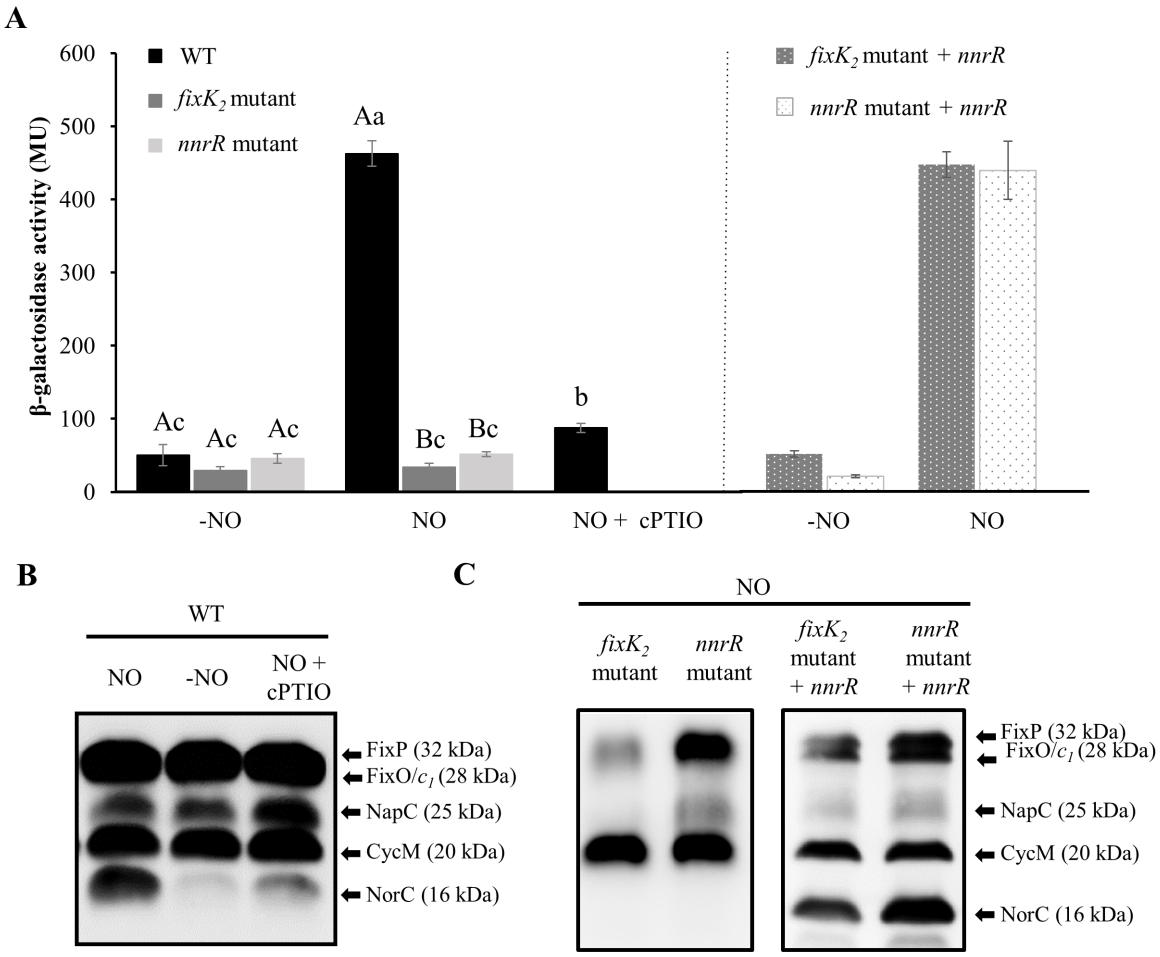
A
β-galactosidase activity (MU)
600
500
400
300
200
100
0
WT
fixK2 mutant
nnrR mutant
fixK2 mutant + nnrR
nnrR mutant + nnrR
Ac
Ac
Ac
Aa
Bc
Bc
b
-NO
NO
NO + cPTIO
-NO
NO
B
WT
NO
-NO
NO + cPTIO
FixP (32 kDa)
FixO/c1 (28 kDa)
NapC (25 kDa)
CycM (20 kDa)
NorC (16 kDa)
C
NO
fixK2 mutant
nnrR mutant
fixK2 mutant + nnrR
nnrR mutant + nnrR
FixP (32 kDa)
FixO/c1 (28 kDa)
NapC (25 kDa)
CycM (20 kDa)
NorC (16 kDa)

Fig. 1

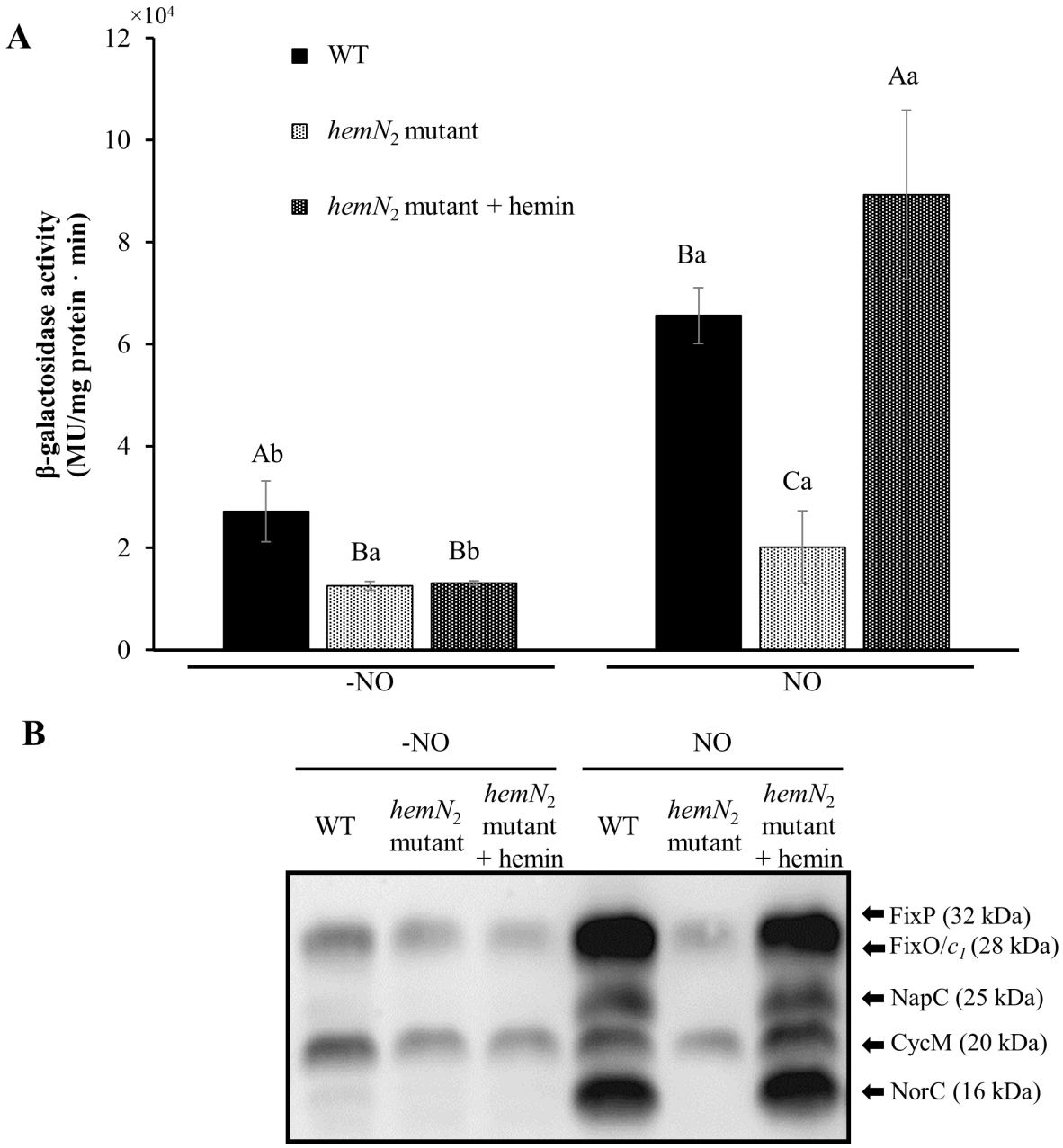

925

926 **Fig. 2**

927

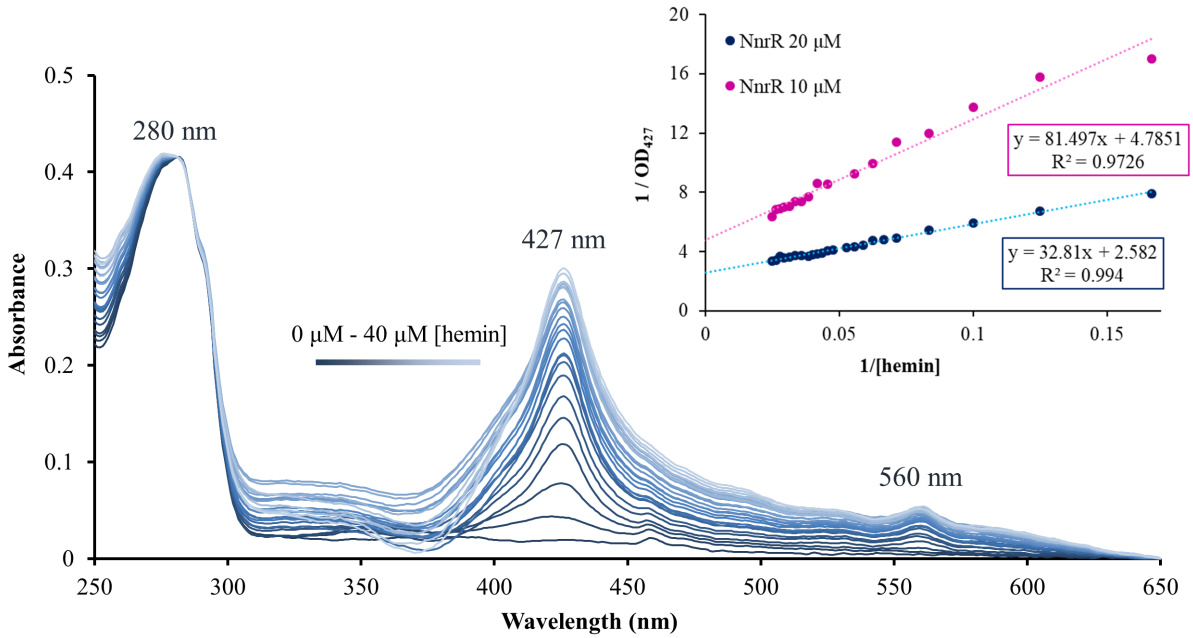

928

929 **Fig. 3**

930

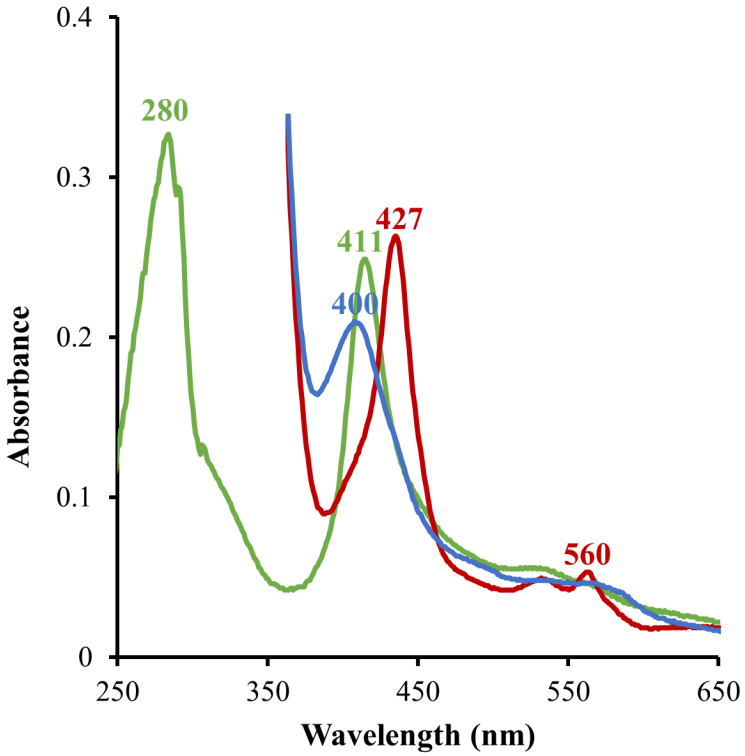

931

932 **Fig. 4**

933

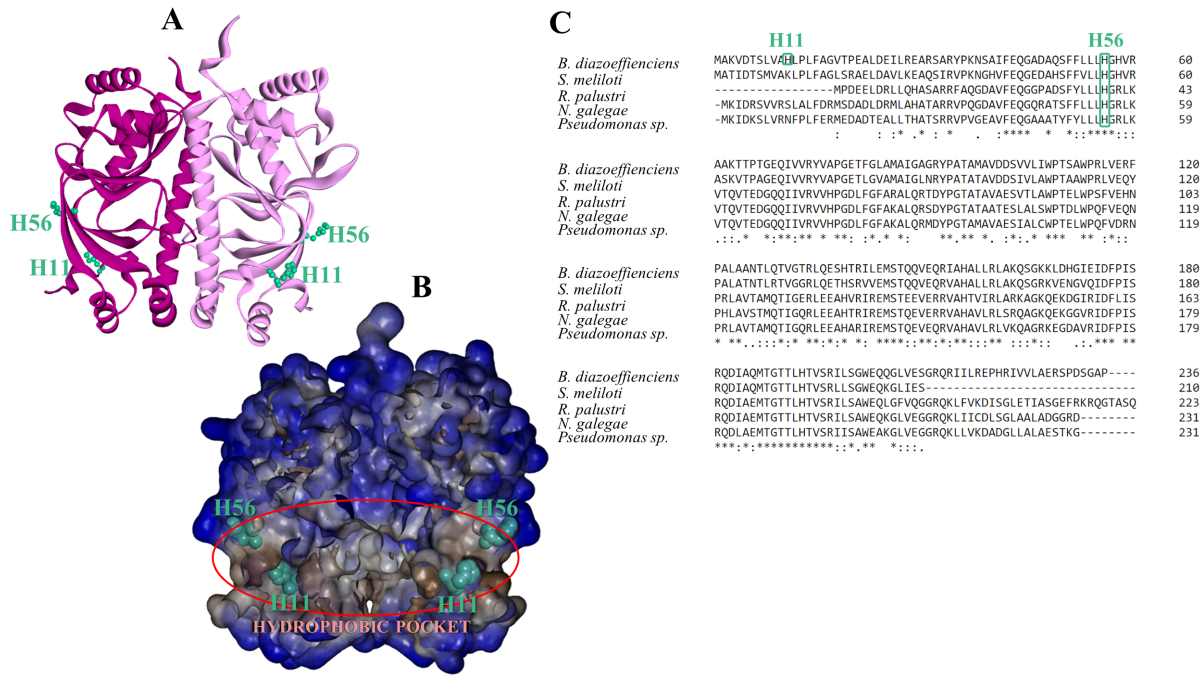

934

935 **Fig. 5**

936

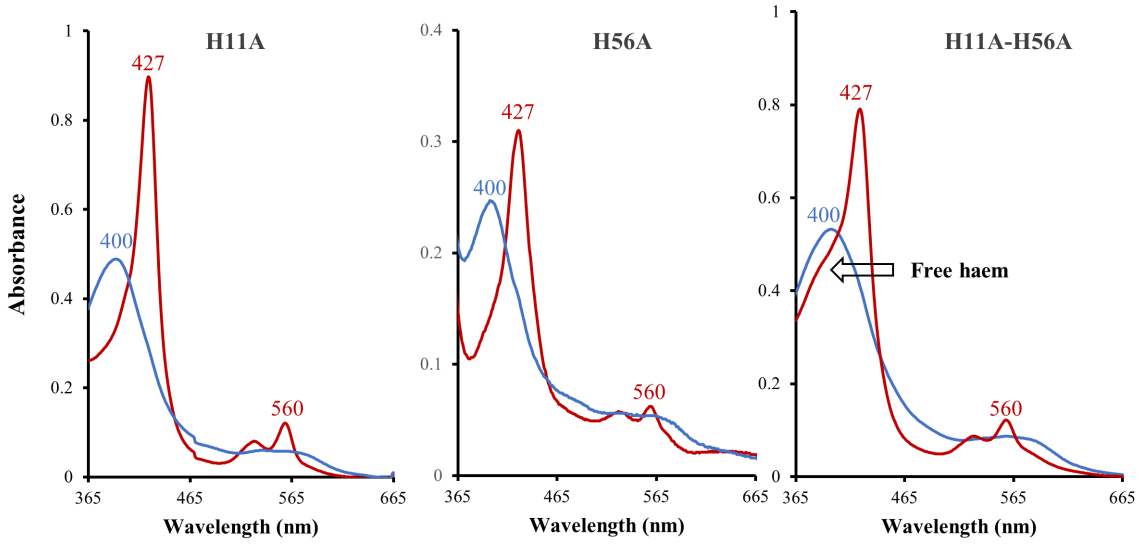

937

938 **Fig. 6**

939

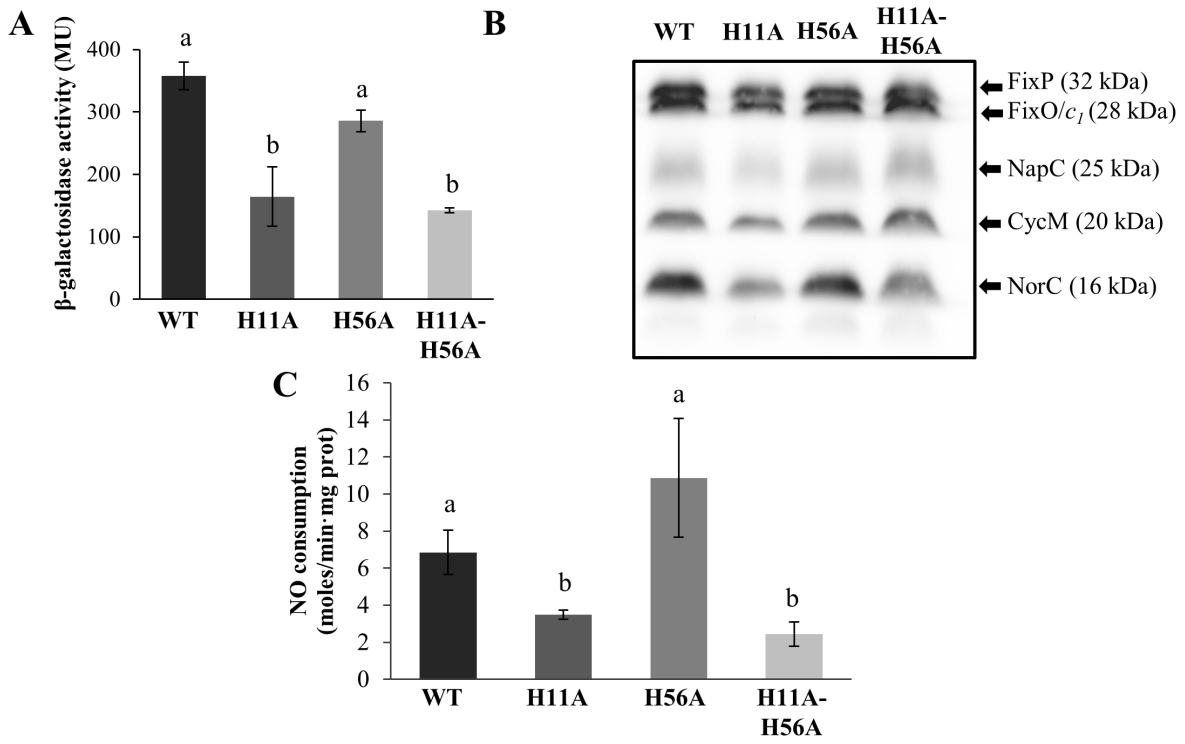

940

941 **Fig. 7**

942

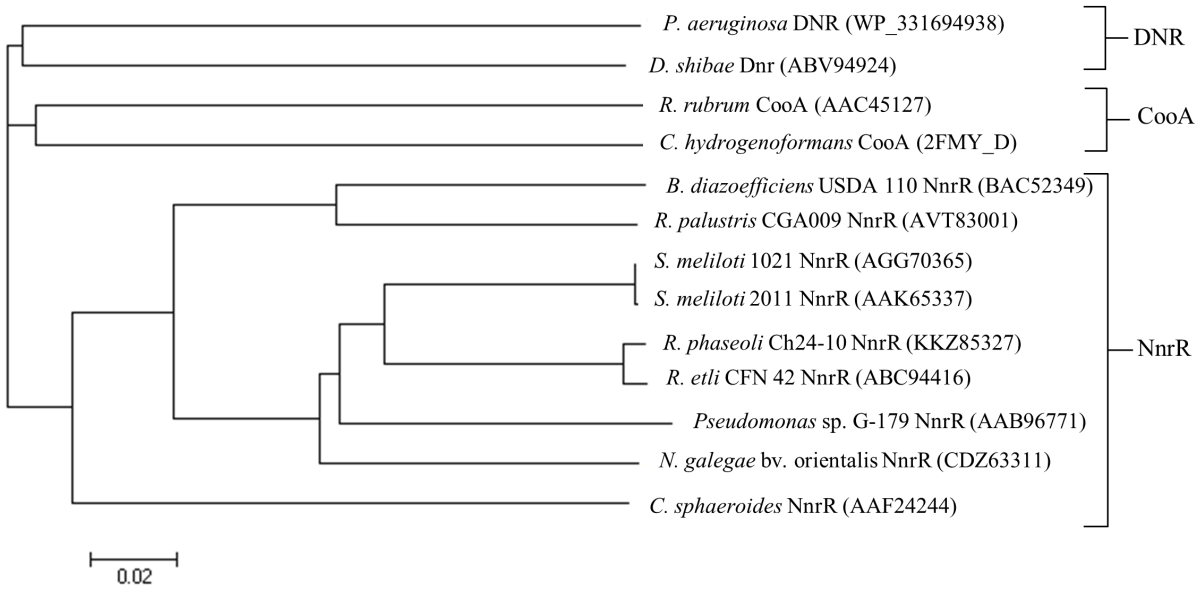

943

944 **Fig. 8**

945

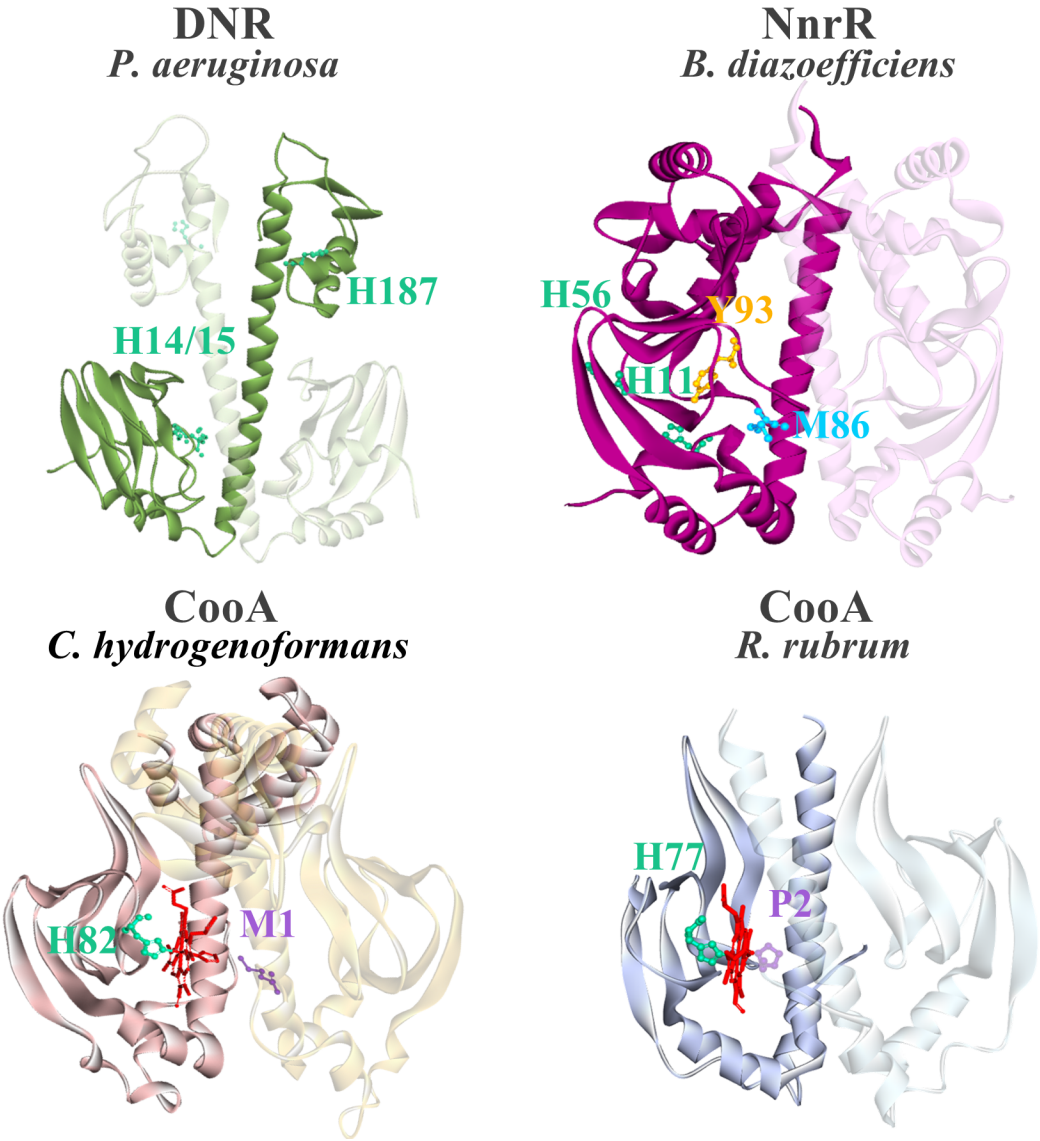

946

947 **Fig.9**

948

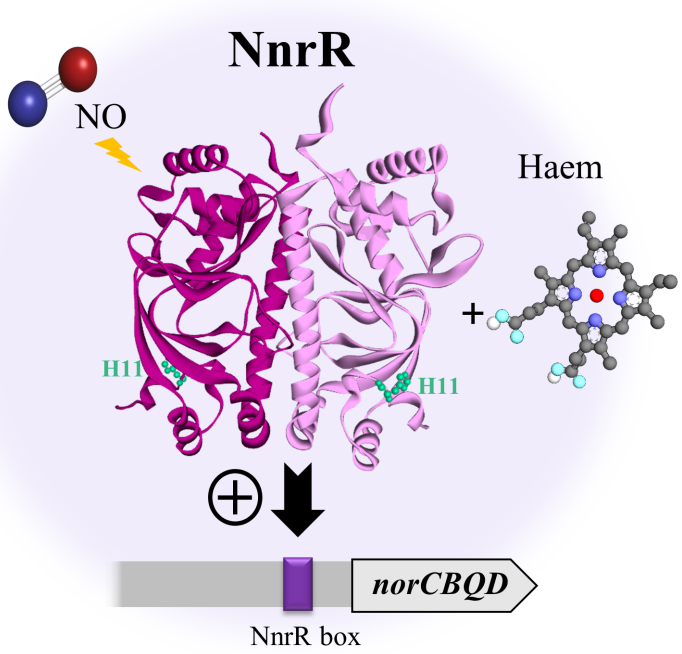

Graphical Abstract